JOURNAL OF MATERIALS SCIENCE **39** (2004) 2443–2449

Crystallization kinetics of Si-TCP bioceramic films

A. PIETAK*, M. SAYER, M. J. STOTT
Department of Physics, Queen's University, Kingston, ON K7L 3N6, Canada
E-mail: alexis@physics.queensu.ca

The crystallization kinetics leading to the formation of a characteristic globular, interconnected morphology in the transformation of an unfired hydroxyapatite precipitate (HA) to silicon stabilized tri-calcium phosphate (Si-TCP) are examined by rapid thermal processing of thin films prepared on silica substrates. The results are interpreted using an Avrami model in which nucleation of Si-TCP is induced by diffusion of a silicon front from the substrate. The model is supported through SEM inspection of the morphological development. The transformation is characterized as an interfacial reaction with Avrami exponent $m = 1.3 \pm 0.2$, activation energy for the reaction $E_c = 2.5 \pm 0.3$ eV and time constant $\tau_c = 20 \pm 1$ s at 950°C. Silicon in the films acts to nucleate Si-TCP, while also causing impurity pinning of grains, resulting in a fine microstructure when excess Si is present in the film.

1. Introduction

Calcium phosphate based bioceramics, notably calcium hydroxyapatite, are well recognized for their bioactive nature [1]. Silicon stabilized tricalcium phosphate (Si-TCP) is an exceptional bioceramic in both bulk and coating forms [2, 3] as it participates in the full remodeling process of bone, recruiting the activity of both bone building (osteoblast) and bone resorbing (osteoclast) cells [3]. Si-TCP has a unit cell akin to that of the high temperature (>1200°C) α-TCP phase and is formed when a colloidal precipitate of calcium hydroxyapatite ($Ca_5(OH)(PO_4)_3$-HA) is sintered in the presence of silicon (Si) or silica (SiO_2) at temperatures between 850–1000°C [2, 4]. The significance of the presence of Si or SiO_2 in the firing of HA was initially recognized when HA films were fired on quartz (SiO_2) substrates [2], resulting in a phase composition consisting of a mixture of HA and Si-TCP, with the characteristic interconnected globular crystal morphology shown in Fig. 1. Both a high phase composition (~75%) of Si-TCP and the characteristic crystal morphology have been identified as factors required for resorptive bioactivity.

This paper describes the use of rapid thermal processing methods to examine the kinetics of the HA → Si-TCP transformation in nano-crystalline HA films fabricated on quartz substrates. An Avrami model of the phase transformation has been employed to guide the interpretation of the results. In conventional Avrami theory, nucleation of a new phase is assumed to follow a power law expression, providing a linear relationship between the Avrami exponent and the kinetics of grain growth and nucleation [5]. This nucleation model does not effectively describe the thin film Si-TCP system on a quartz substrate, and a model based on heterogeneous nucleation controlled by diffusion of a Si front from the substrate has been developed. This model may apply to similar thin film systems where a new phase is generated as a result of impurity diffusion from the substrate.

2. Experiment

2.1. Unsintered film fabrication

Thin films of an HA nano-crystalline precipitate on quartz substrates were created by dip coating the substrate with a colloidal sol formed by reaction in an ammoniated aqueous mixture. Details of the chemical preparation have been given by Langstaff *et al.* [2, 4]. Scanning electron microscope examination of the cross-section of representative films after deposition and drying showed that the film thickness was 1.2 ± 0.2 μm. Silica doped sols were prepared by addition of a fumed silica (SiO_2) Cab-o-Sperse™ SiO_2 powder (20 nm mean diameter) to the HA sol prior to depositing the film [2]. Doping concentrations were 0.3:1 and 1:1 molar ratios of SiO_2 to HA.

2.2. Film processing

The crystallization kinetics of the phase transformation at anneal temperatures of 850, 900, 950 and 1000°C respectively were examined through rapid thermal processing using an AG Associates Model 410 Rapid Thermal Processor. The coated quartz substrate was placed on a silicon process wafer. Rapid heating rates (50°C/s) controlled by the temperature of the process wafer, precise temperature control (<1% variability in temperature) and quench cooling conditions (−60°C/s) from 1000 to 700°C generated 'snapshot' samples of the HA → Si-TCP transformation as a function of

*Author to whom all correspondence should be addressed.

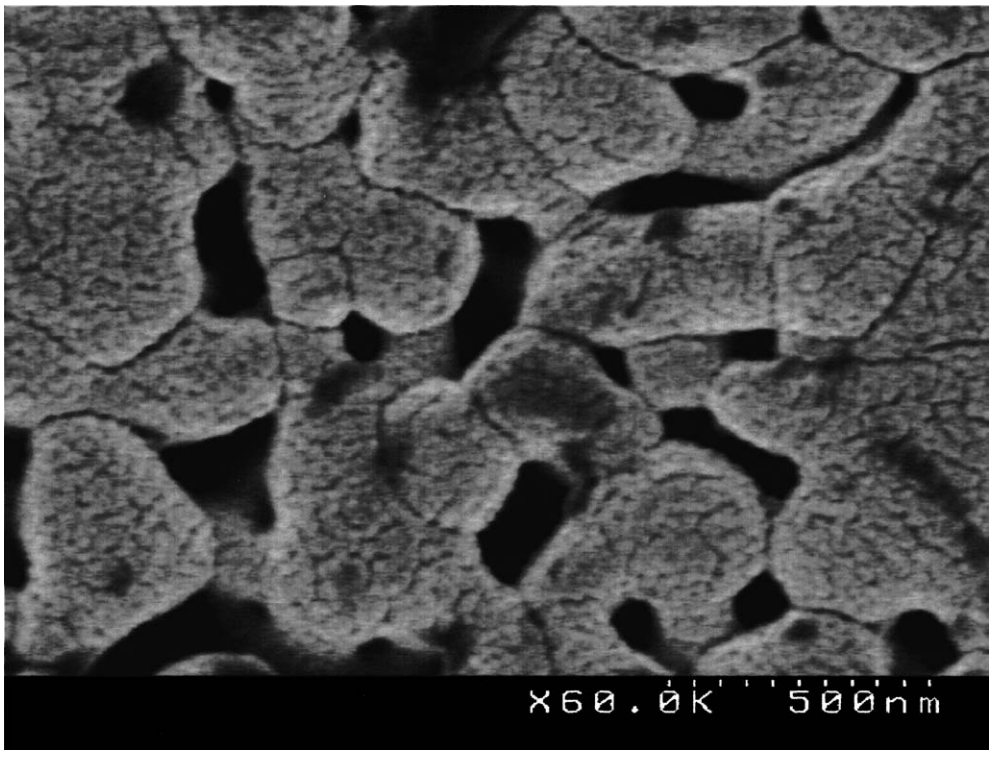

Figure 1 Planar view of typical thin film microstructure, detailing porous, interconnected morphology. Micrographs such as this are used to estimate the average grain radius of a sample.

temperature and time. Attaching a thermocouple to the surface of a representative sample checked the temperature of the samples during processing. The sample temperature was at the temperature of the silicon process wafer to within 10°C, and remained so throughout the course of a 120 s anneal.

2.3. High resolution field emission scanning electron microscopy

A Hitachi S-4500 field emission scanning electron microscope was used to investigate microstructure within the fired coating. Samples were prepared by sputtering gold to a thickness of ∼10–50 Å. This coating was observed as a granular texture visible on the grains of the sample.

2.4. Phase composition

The volume fractions of the crystalline phases present were determined using glancing angle X-ray diffraction (GA-XRD) [6]. All GA-XRD spectra were obtained with a 12 kW Rigaku rotating anode diffractometer fitted with a chromium (Cr) target, with a glancing angle (GA $= \theta$) of 2°. The volume fraction of the Si-TCP phase was calculated by normalizing the sum of the integrated area of G-XRD peaks representative of Si-TCP to the sum of integrated areas of representative G-XRD peaks of the phase mixture consisting of HA, β-TCP and Si-TCP:

$$V(T,t) = \frac{\sum \text{SiTCP}}{\sum \text{HA} + \sum \beta\text{TCP} + \sum \text{SiTCP}} \qquad (1)$$

2.5. X-ray photoelectron spectroscopy (XPS)

The concentration of Si at the surface of the film was determined using XPS spectroscopy. XPS was performed on a Leybold Max 200 with mono-energetic Al K_α X-rays with energy 1486.6 eV. Argon etching was used to obtain a measurement ∼10 nm from the surface of the film to avoid surface contamination. Identification of Si was based on the release of photoelectrons with characteristic energy in the range of 96.7–112.7 eV.

2.6. Grain radius estimation

Grain radius was estimated from SEM micrographs such as that shown in Fig. 1. The true area of crystalline and porous regions was estimated on the basis of light and dark areas of the micrograph, corresponding to grain and porous area, respectively. The number of grains in the picture, n, was manually counted, and the average radius of the grain, r, was estimated by assuming grains form circular cross sections in the 2D plane:

$$r = \sqrt{\frac{\text{Crystalline Area}}{n\pi}} \qquad (2)$$

3. Results and analysis

3.1. Crystallization kinetics

The measured volume fraction of the Si-TCP phase developed as a function of time for hold temperatures from 850 to 1000°C, $V(t, T)$, are shown for undoped sols in Fig. 2. The transformation kinetics of the HA → Si-TCP transformation are well described by the

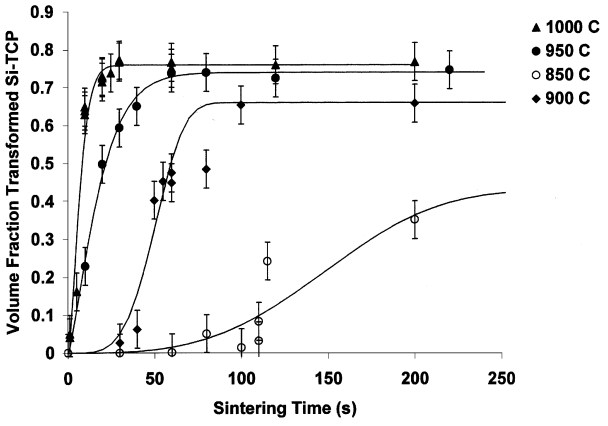

Figure 2 HA → Si-TCP phase transformation for undoped sols for temperatures of 850–1000°C.

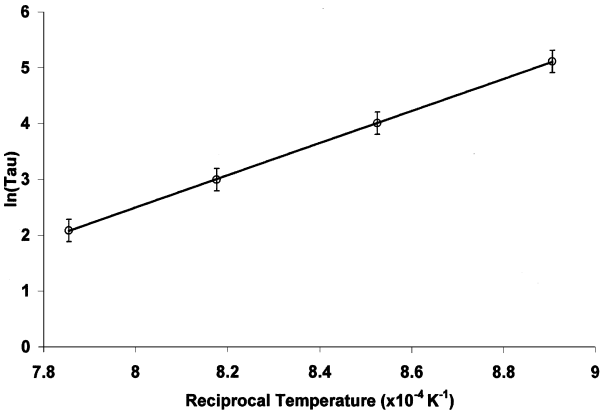

Figure 3 Estimation of reaction activation energy from plot of ln(τ) vs. reciprocal temperature.

Avrami equation:

$$V = A\left(1 - \exp\left(-\left(\frac{t}{\tau}\right)^{m}\right)\right) \tag{3}$$

where m is the Avrami exponent and A is the equilibrium fraction of Si-TCP in the resulting sintered sample. The transformation with characteristic time (τ is assumed to be thermally activated:

$$\tau = \tau_o \exp(E_a / k_B T) \tag{4}$$

with activation energy E_a, τ_o the characteristic time of the transformation in the high temperature limit, and k_B the Boltzman constant.

Fitted values of m, A, and τ for the HA → Si-TCP transformation at various temperatures are listed in Table I. Noteworthy are the unusually small (<1.5) values of the Avrami exponent m for undoped films sintered at temperatures between 850–950°C. As outlined in the proceeding analysis, these low Avrami exponents have non-physical interpretations, suggesting that the conventional Avrami nucleation model may not be appropriate for this system. The plot of ln(τ) vs. 1/T shown in Fig. 3 exhibits a linear relationship and yields the activation energy $E_a = 2.49 \pm 0.05$ eV.

SEM inspection indicates rapid, linear grain growth at temperatures of 950 and 1000°C, as depicted in Fig. 4. Earlier TEM cross-section data for Si-TCP thin films showed single crystal globular grains that had grown in all three dimensions [7]. Spherical, linear grain growth has therefore been attributed to Si-TCP grains in the description of the extended transformed volume fraction of the Avrami model described below. TEM cross-section data also depicts small grains of residual HA phase (15–20 nm diameter) near the film-substrate interface [7].

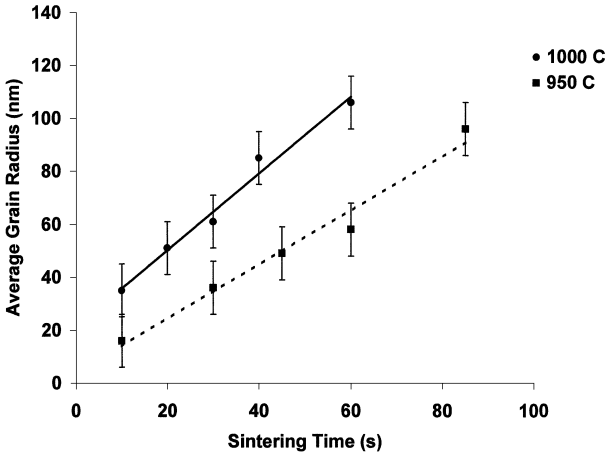

Figure 4 Grain growth of Si-TCP at 950 and 1000°C. Linear grain growth is observed in thin films early in the transformation.

An equivalent expression for the Avrami equation is a statement in terms of the extended and actual transformed volume fractions, V_{ext} and V, respectively [5, 8, 9]:

$$V = A(1 - \exp(-V_{ext})) \tag{5}$$

where 'extended' denotes the transformed volume had grain growth been unimpeded by impingement upon neighboring grains. The extended transformed volume for spherical grains of radius r, growing in a film of

TABLE I Summary of fitting parameters of the Avrami model, Equation 11

Temperature (°C)	Additional silica doping mol Si: mol HA	Equilibrium volume fraction Si-TCP: $A(T)$%	Reaction time constant: τ (s)	Avrami exponent (m)
850	Undoped	(43 ± 4)	(166 ± 5)	(0.9 ± 0.3)
900	Undoped	(70 ± 3)	(55 ± 2)	(1.14 ± 0.4)
950	Undoped	(75 ± 4)	(20 ± 1)	(1.30 ± 0.2)
1000	Undoped	(77 ± 1)	(8 ± 1)	(2.94 ± 0.2)
950	0.3:1	(75 ± 3)	(3.75 ± 0.2)	(0.46 ± 0.1)
950	1:1	(78 ± 3)	(0.24 ± 0.1)	(0.21 ± 0.1)

thickness L and planar area w^2, is given by:

$$V_{\text{ext}} = \frac{\int_o^t \frac{4}{3}\pi r^3 \frac{\partial n}{\partial s}\text{d}s}{Lw^2} \tag{6}$$

where $\frac{\partial n}{\partial s}$ describes the rate of nucleation of the new phase at time s.

Since it has been determined that grains are spherical and grow linearly, the only parameter that is not experimentally accessible in this system is the nucleation rate. Nucleation models usually assume a power law expression [5]:

$$\frac{\partial n}{\partial t} = n_{\text{o}} a t^{\text{a}-1} \tag{7}$$

where n_{o} is the number of nucleates at the beginning of the transformation, and 'a' is a parameter describing a constant ($a = 1$), increasing ($a > 1$) or decreasing ($a < 1$) nucleation rate. Using (5), (6) and (7), the total time dependence of the extended volume, described by the Avrami exponent m, can be directly related to both the kinetics of nucleation and the kinetics and dimension of grain growth. For spherical, linear grain growth with grain boundary velocity U, the grain radius after sintering for time 't' is:

$$r = Ut \tag{8}$$

and the extended transformed volume fraction for sintering for time t is:

$$V_{\text{ext}} = \frac{\int_o^t \frac{4}{3}(U^3(t-s)^3)(an_{\text{o}}s^{\text{a}-1})\text{d}s}{Lw^2} \propto t^{3+\text{a}} \tag{9}$$

Comparing (9) with (2) we find that for linear spherical grain growth with a power law expression for the nucleation kinetics, the Avrami exponent 'm' is related to the nucleation parameter 'a' via:

$$m = a + 3 \tag{10}$$

However, for the HA $\rightarrow$ Si-TCP transformation, characterized by spherical, linear grain growth, with an Avrami exponent of $m = 1.3 \pm 0.2$ at 950°C, this leads to a nucleation parameter $a = -1.7 \pm 0.3$. This strongly negative value is non-physical, implying the disappearance of Si-TCP seed nuclei as the reaction proceeds. The situation is similar for the 900 and 850°C transformation and for the doped film data, all of which are described by $m < 3$. Clearly, the conventional power law description of the time dependence of nucleation stated in Equation 7, does not describe the thin film Si-TCP system appropriately. A modified description of the nucleation kinetics of the Si-TCP film system is developed in the subsequent analysis.

In studies of the formation of Si-TCP in powders it has been shown that the presence of Si is necessary to form the TCP phase at $T < 1200$°C [4]. In the film samples no silicon is initially present in the coating material, but diffusion of Si is likely to occur during firing. A model of nucleation controlled by an advancing front of Si has therefore been developed. It is assumed that a critical concentration of Si, C_{ct}, is required to induce the formation of a nucleus of Si-TCP. As the critical concentration of Si advances from the substrate, Si-TCP grains nucleate and grow. Therefore, the nucleation rate of Si-TCP is proportional to the rate of advancement of an iso-concentration of Si diffusing from the substrate. The expression for the extended volume fraction of Si-TCP in the thin film now becomes:

$$V_{\text{ext}} = \frac{\int_{\text{o}}^t \frac{4}{3}\pi(U^3(t-s)^3)\left(\rho_{\text{TCP}}\frac{\partial x_{\text{ct}}}{\partial s}\right)\text{d}s}{L} \tag{11}$$

where $\frac{\partial x_{\text{ct}}}{\partial s}$ is the rate of advancement of the critical concentration of Si, and ρ_{TCP} is a scaling factor representing the density of Si-TCP nuclei forming per unit area swept out by the critical front of Si.

3.2. Diffusion of silicon

The atomic concentration of Si near the surface of Si-TCP films sintered at 1000°C for various periods of time was measured by XPS. Thickness of the thin film was estimated directly from FE-SEM of a cross section of thin film. The results are displayed in Fig. 5 for undoped films of estimated thickness 1.2 ± 0.2 μm. Note in Fig. 5 that diffusion of Si is rapid in the initial stages of the transformation from 30 s to 5 min, at which point it reaches an initial equilibrium value of about 1.0 atm% Si between 15 min and 1 h. After sintering for 16 h, the Si concentration has increased significantly to 2.9 atm% Si. The initial plateau of Si, and the subsequent increase in Si concentration after very long time periods are interpreted as the results of diffusion occurring via two diffusion paths: a high diffusivity path with low saturation dominating the early stages of the reaction occurring along single crystal grain surfaces and boundaries, and a low diffusivity path with higher saturation occurring through the bulk of the single crystal grain.

The diffusion equation for the concentration of Si, $C(x, t)$, at position x in the thin film and at time t is

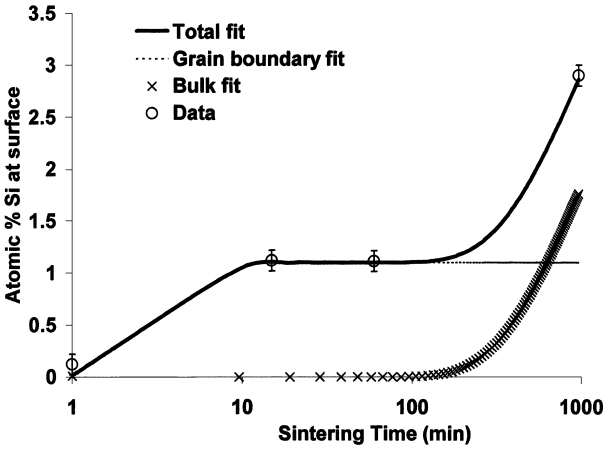

Figure 5 Estimating Si diffusion through the film from Si concentration at the surface of undoped films as a function of time determined using XPS spectroscopy.

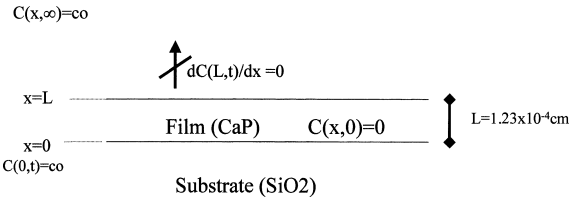

Figure 6 Thin film geometry, indicating diffusion of Si from substrate, with associated boundary conditions.

[10]:

$$\frac{\partial^2 C}{\partial x^2} = \frac{1}{D}\frac{\partial C}{\partial t} \tag{12}$$

The geometry, boundary and initial conditions are displayed in Fig. 6, where the film is in the y-z plane, $x = 0$ is the film-substrate interface and $x = L$ is the film-atmosphere interface. The concentration of Si in the thin film is modeled as the linear combination of a steady state and positive definite transient solution, c_o and $c(x, t)$, respectively:

$$C(x, t) = c_o - c(x, t) \tag{13}$$

Initially at time $t = 0$ the Si concentration in the film is taken to be zero. Subsequently, the concentration at the film-substrate interface is taken to be c_o, the solid solubility limit, with zero flux at the film-atmosphere interface. At long times, a uniform concentration, c_o, is established in the film. Consequentially, the initial condition is $C(x, t = 0) = 0$, the boundary conditions are $\frac{\partial C(x,t)}{\partial x}\ |_{x=L} = 0$ and $C(x = 0, t) = c_o$, and the steady state is $C(x, t \to \infty) = c_o$.

The solution of (13) for the described conditions is:

$$C(x, t)_\Delta = C_{o\Delta}\left(1 + \sum_{n=0}^{\infty}\left(\frac{2}{Lk}\right)(\sin(kx))\exp(-k^2 D_\Delta t)\right)$$

$$k = (n + 1/2)\frac{\pi}{L} \tag{14a}$$

where Δ indicates either grain boundary (gb) or bulk (b) diffusion mechanism, D is the diffusion constant, c_o is the saturation value of silicon in either diffusion mechanism, and L is the film thickness. The total concentration of Si is the sum of grain boundary and bulk diffusion:

$$C(x, t) = C(x, t)_{gb} + C(x, t)_b \tag{14b}$$

The fit of (14b) to the data provides an estimate for the values of c_{ogb}, D_{gb}, c_b, and D_b for silicon in the thin film system as listed in Table II. It is assumed that the phase transformation from HA → Si-TCP requires Si substitution into the bulk crystal of HA/Si-TCP, and therefore, only bulk diffusion parameters will be considered in the subsequent analysis.

TABLE II Estimates of diffusion parameters derived from fit of surface silica concentration to thin film diffusion Equation 12, with a film thickness of (1.2 ± 0.2) μm

Path of diffusion	Diffusion co-efficient (cm^2/s)	Saturation level (atm.%)
Grain boundary	$(2 \pm 0.5) \times 10^{-9}$	1.10 ± 0.20
Grain bulk	$(6 \pm 2) \times 10^{-12}$	3.5 ± 0.7

3.3. Diffusion controlled nucleation Avrami model (DCN Avrami model)

The concentration distribution of Si in the thin film for the time period of the HA → Si-TCP transformation at 950°C (1–200 s) was calculated using Equation 14a, assuming bulk diffusion. The calculation used the bulk diffusion co-efficient and saturation value at 950°C, listed in Table II. The rate of advance of a concentration front of Si was determined numerically as a function of the critical concentration C_{ct}. The results were used to describe the transformation at 950°C within the diffusion controlled Avrami model incorporating Equations 5 and 11. In the model the velocity of grain growth $U = 1.0 \pm 0.1$ nm/s was obtained from observed grain growth at 950°C, plotted in Fig. 4. C_{ct} and ρ_{TCP} were treated as free parameters. The best fit to the volume fraction of transformed Si-TCP at 950°C using Equations 5 and 11 is shown in Fig. 7, obtained for $C_{ct} = 0.3 \pm 0.2$ atm% and $\rho_{TCP} = (1 \pm 2) \times 10^{16}$ nucleates/cm^3.

Unfortunately, due to a lack of Si diffusion information, $C(x, t)$ could not be calculated at other temperatures, or in the case of Si doped films. In general, the advance of a critical front of Si in the thin film can be described by:

$$x_{ct} = \frac{p_1 t}{(p_2 + t)} + \frac{p_3 t}{(p_4 + t)} \tag{15}$$

where p_1–p_4 are fitted parameters.

Addition of particulate silica to the thin films prior to sintering enhances the rate of Si-TCP phase development as illustrated in Fig. 8. Doped films also exhibit exceptionally low Avrami exponents, listed for 0.3:1

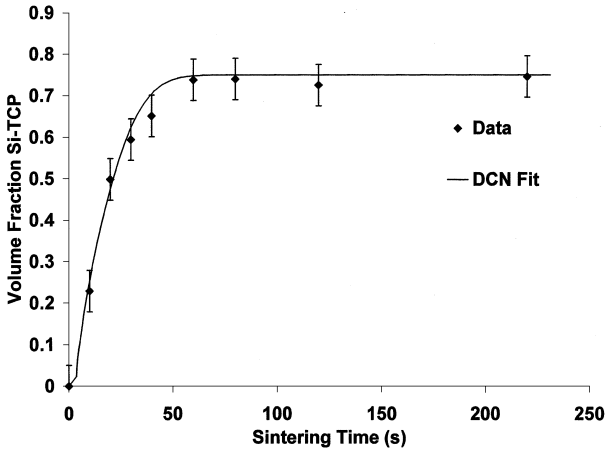

Figure 7 Diffusion controlled nucleation (DCN) fit to transformation at 950°C using observed grain growth and diffusion parameters at 950°C.

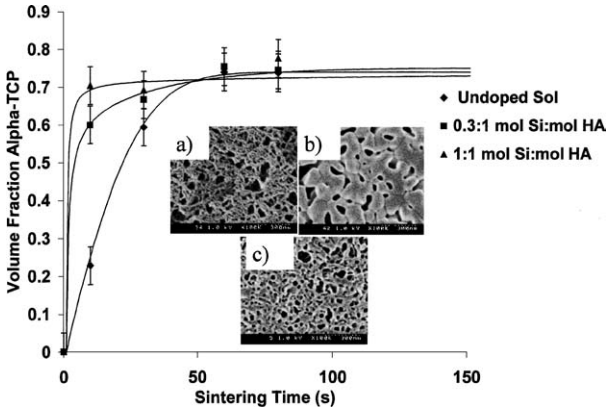

Figure 8 Rate of phase transformation increases in silica particle doped films, while morphology is pinned (inset). Pinning of the microstructure is evident in the 1:1 mol SiO_2: mol HA sample, inset (c), sintered for 60 s at 950°C. This has a microstructure similar to that of the unsintered film, inset (a). In the undoped sintered sample, inset (b), extensive grain growth has occurred, resulting in interconnected grains of Si-TCP. Diffusion controlled nucleation (DCN) fit to transformation is shown.

and 1:1 doped films in Table I, which as discussed earlier have non-physical interpretations under the conventional nucleation model.

While the addition of particulate silica changes the diffusion geometry of the undoped film system outlined in Fig. 6, a simple interpretation regarding the role of silica in the development of phase and morphology of Si-TCP can be obtained by calculating and comparing the nucleation rate, using Equation 15 for the 0.3:1, 1:1 and undoped films sintered at 950°C using the DCN Avrami model. Fig. 8 details the DCN Avrami fit for 0.3:1, 1:1 mol Si:HA doped films and undoped films, all sintered at 950°C. The nucleation kinetics of the 0.3:1, 1:1 and undoped films sintered at 950°C, shown in Fig. 9, were calculated to give the best fit of the DCN Avrami model with the observed grain growth rates for the respective film series. The nucleation kinetics indicate increasing nucleation rates of Si-TCP with increasing SiO_2 particulate addition to the thin film.

The inset to Fig. 8 displays grain growth inhibition for excessive silica content. Pinning of the microstructure is evident in the 1:1 mol SiO_2: mol HA sample, (c), sintered for 60s at 950°C. This has a microstructure similar to that of the unsintered film, (a). In the undoped sintered sample, (b), extensive grain growth has

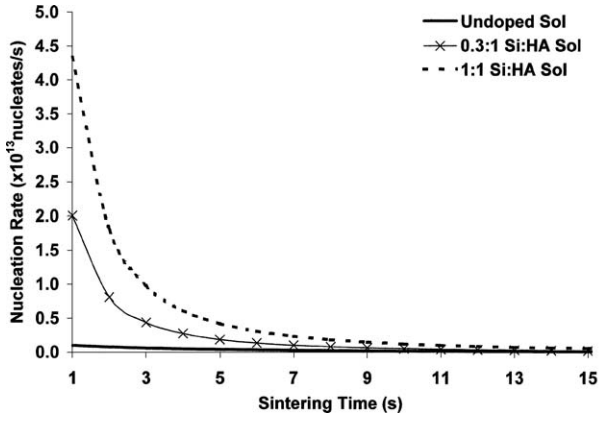

Figure 9 Nucleation rate increases in silica particle doped films.

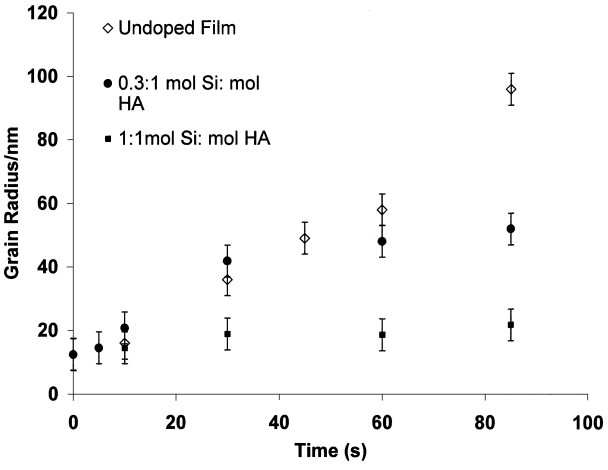

Figure 10 Grain growth of Si-TCP in doped and undoped films at 950°C.

occurred, resulting in interconnected grains of Si-TCP. Fig. 10 shows that the rate of grain growth decreases with the Si content of the film.

4. Discussion

The results indicate that the HA → Si-TCP transformation is well described by a modified Avrami model involving diffusion-controlled nucleation. Silica acts as a nucleation agent for the Si-TCP phase in the thin film. Comparison of nucleation rates calculated for undoped and doped films in Fig. 9 support this interpretation as increasing silica concentration in the film result in an increase in the nucleation rate.

The morphological development of undoped Si-TCP thin films is characterized by rapid linear grain growth, which leads to a coarse grained, interconnected microstructure. The interconnected microstructure implies the coalescence of impinging grains. This is in conflict with a normal grain growth mechanism, where impinging grains cease growth at a common interface [11]. The addition of excess silica by doping the film leads to progressive inhibition of grain growth with increasing silica concentration.

It is suggested that Si acts as a grain boundary pinning impurity in the HA/Si-TCP thin film system. Trace levels of Si present in the film through diffusion from a SiO_2 substrate lead to weak pinning of the initial HA microstructure. Si induces the nucleation of Si-TCP phase, which having some energy advantage over HA, grows preferentially. The resulting microstructure consists of large interconnected grains of Si-TCP, with residual fine grained HA remaining at the film-substrate interface [7, 12]. When excess silica is added as a dopant, although more grains are nucleated, the grain boundary mobility of both HA and Si-TCP phases is decreased, and as a result grain growth is progressively slowed, Fig. 10.

5. Conclusions

Silicon nucleates Si-TCP in the thin film system. This conclusion is supported by a model of nucleation controlled by diffusion of an impurity from a substrate into a thin film. The generation of a highly interconnected

microstructure in undoped films is the result of rapid linear grain growth of Si-TCP with coalescence of grains, which occurs for low levels of silica at grain boundaries. Further addition of silica particulate to the thin film leads to Si impurity pinning of grain boundaries, resulting in a much finer grained microstructure. The HA $\rightarrow$ Si-TCP transformation is parameterized by an Avrami exponent which varies from $m = 0.9$ to 2.9 for reactions at $T = 850$ to 1000°C, and an activation energy for the entire transformation, $E_a = (2.49 \pm 0.05)$ eV.

These results are derived from thin film geometry, which has clear mathematical advantages for the development of a comprehensive diffusion controlled nucleation model. However, an analogous nucleation and growth model may occur in a three dimensional bulk ceramic system, in which silica diffuses from silica particles dispersed through a calcium phosphate matrix.

Acknowledgements

This work was supported through a Collaborative Research and Development Grant of the Natural Sciences and Engineering Research Council of Canada and Millenium Biologix Inc., Kingston, ON.

References

1. K. DE GROOT, C. KLEIN and J. WOLKE, in "CRC Handbook of Bioactive Ceramics," edited by T. Yamamuro, L. Hench, and J. Wilson (CRC Press, Boca Raton, Florida, 1989).
2. S. D. LANGSTAFF, M. SAYER, T. J. N. SMITH, S. M. PUGH, S. A. M. HESP and W. T. THOMPSON, *Biomaterials* **20** (1999) 1727.
3. Q. QIU, P. VINCENT, B. LOWENBERG, M. SAYER and J. E. DAVIES, *Cells and Mater.* **3** (1993) 351.
4. S. LANGSTAFF, M. SAYER, T. J. N. SMITH and S. M. PUGH, *Biomaterials* **22** (2001) 135.
5. S. RANGANATHAN and M. VON HEIMENDAHL, *J. Mater. Sci.* **16** (1981) 2401.
6. E. HOROWITZ and J. E. PARR (eds.), "Performance of Calcium Phosphate Coatings for Implants," ATSM Publication Code 04-011960-54 (Philadelphia, 1994).
7. M. SAYER, A. STRATILATOV, S. D. LANGSTAFF, J. REID, L. CALDERIN, M. J. STOTT, T. J. N. SMITH and J. A HENDRY, *Biomaterials* **24** (2003) 369.
8. M. AVRAMI, *J. Chem. Phys.* **9** (1941) 177.
9. *Idem.*, *ibid.* **8** (1939) 212.
10. P. SHEWMON, "Diffusion in Solids" (McGraw-Hill, Toronto, 1963).
11. P. COTTEREL and P. MOULD, "Recrystallization and Grain Growth in Metals" (John Wiley & Sons, New York, 1976).
12. S. LANGSTAFF, M. SAYER, L. WEAVER, S. PUGH and T. SMITH, *Mater. Res. Soc. Symp. Proc.* **414** (1996) 87.

Received 22 January
and accepted 8 October 2003